

Phase Behavior and Mesophase Structures of 1,3,5-Benzene- and 1,3,5-Cyclohexanetricarboxamides: Towards an Understanding of the Losing Order at the Transition into the Isotropic Phase

Andreas Timme,^[a] Roman Kress,^[a] Rodrigo Q. Albuquerque,^[b] and Hans-Werner Schmidt*^[a]

Abstract: One of the simplest and most-versatile motifs in supramolecular chemistry is based on 1,3,5-benzenetricarboxamides. Variation of the core structure and subtle changes in the structures of the lateral substituents govern the self-assembly and determine the phase behavior. Herein, we provide a comprehensive comparison between the phase behavior and mesophase structure of a series of 1,3,5-benzene- and 1,3,5-cyclohexanetricarboxamides that contain linear and branched alkyl substituents. Depending on the substituent, different crystalline,

plastic crystalline, and liquid crystalline phases were formed. The relatively rare columnar nematic (N_C) phase was only observed in cyclohexane-based trisamides that contained linear alkyl substituents. Of fundamental interest in liquid crystalline supramolecular systems is the transition from the mesomorphic state into the isotropic state and, in particular, the question of how

the order decreases. Temperature-dependent IR spectroscopy and XRD measurements revealed that columnar H-bonded aggregates were still present in the isotropic phase. At the clearing transition, mainly the lateral order was lost, whilst shorter columnar aggregates still remained. A thorough understanding of the phase behavior and the mesophase structure is relevant for selecting processing conditions that use supramolecular structures in devices or as fibrillar nanomaterials.

Keywords: liquid crystals • self-assembly • structure elucidation • thermal analysis • X-ray diffraction

Introduction

A variety of compounds that are composed of disk-like molecules are known to form liquid crystalline (LC) mesophases. The first series of such compounds, which consisted of hexakis(alkanoyloxy)benzenes, was reported by Chandrasekhar et al. in 1977.^[1] Another series of compounds, which consisted of 1,3,5-benzenetricarboxamides with certain alkyl substituents, was reported by Matsunaga et al. to exhibit thermotropic liquid-crystalline behavior over a broad temperature range.^[2,3] Mesophase formation with columnar hexagonal order resulted not only from the anisometry of the

disc-shaped molecules. To a large extent, it was stabilized by the presence of three amide groups per molecule, thereby yielding strong hydrogen bonds, which led to the formation of stable columnar aggregates.^[4–9] Owing to the formation of supramolecular structures, these compounds were capable of forming physical gels of a variety of organic liquids^[10–13] as well as aqueous solutions.^[14,15] These compounds were also applied as functional additives to nucleation and clarification agents for isotactic polypropylene and polyvinylidene fluoride^[16–18] and as additives to improve the electret performance of polypropylene.^[19,20] Bushey et al. described hexa-substituted aromatic cores that consisted of three amide substituents in the 1,3,5-positions that were flanked by substituents other than hydrogen at each of the remaining positions.^[21]

A structurally similar series to 1,3,5-benzenetricarboxamides are 1,3,5-cyclohexanetricarboxamides, first reported by Tomatsu et al.^[22] The different core strongly affected the stacking behavior and thermal properties compared with benzenetricarboxamides.^[23,24] Some of these cyclohexane derivatives were also excellent gel-forming molecules for non-polar organic solvents^[25] and aqueous solutions.^[26–28]

Herein, two series of 1,3,5-tricarboxamides, one with a benzene core and one with a cyclohexane core, with linear and branched alkyl substituents (Table 1) were compared with respect to their phase behavior and mesophase structure to obtain a deeper understanding of the structure–prop-

[a] A. Timme, R. Kress, Prof. Dr. H.-W. Schmidt
Macromolecular Chemistry I
Bayreuther Institut für Makromolekülforschung (BIMF)
and Bayreuther Zentrum für Kolloide und
Grenzflächen (BZKG)
University Bayreuth, 95440 Bayreuth (Germany)
Fax: (+49)921-55-3206
E-mail: hans-werner.schmidt@uni-bayreuth.de

[b] Prof. Dr. R. Q. Albuquerque
Theoretical Physics IV
University Bayreuth, 95440 Bayreuth (Germany)
Current Address: Institute of Chemistry of São Carlos
University of São Paulo, Av. Trab. São Carlense 400
13560-970 São Carlos (Brazil)

Supporting information for this article is available on the WWW under <http://dx.doi.org/10.1002/chem.201103216>.

Table 1. Chemical structures of 1,3,5-tricarboxamides, based on either benzene (1) or cyclohexane cores (2).

1a		2a	
1b		2b	
1c		2c	
1d		2d	
1e		2e	
1f		2f	
1g		2g	
1h		2h	
1i		2i	
1j		2j	
1k		2k	
1l		2l	
1m		2m	
1n		2n	
1o		2o	

erty relationships in these compounds. Although a lot of 1,3,5-benzenetricarboxamides have been synthesized and characterized by Matsunaga et al., not all of their mesophases could be classified at the time.^[2,3] The supramolecular structures of stacked molecules of 1,3,5-benzene- and 1,3,5-cyclohexanetricarboxamides have already been compared by Lightfoot et al., but only one compound of each series that contained short polar substituents was described.^[8]

Special attention was given to the stepwise losing of order during heating at the transition from the mesophase into the isotropic phase. The structure of the nematic phase, which is formed by some 1,3,5-cyclohexanetricarboxamides, was of fundamental interest.^[22] As this phase is an intermediate state in between a higher-ordered columnar phase and the isotropic liquid, it may help to understand what happens at the transition into the isotropic state. Laschat et al. investigated discotic liquid crystals and found that the hexagonal arrangement of the columns was lost in the isotropic melt, but they did not describe what happened to the columns themselves.^[29] Coming from 3D order in the crystalline state, hexagonal or rectangular columnar mesophases were formed at higher temperatures, and possessed two types of

molecular order: First, the stacking along the column axis, caused by strong threefold hydrogen bonding, and, second, the intercolumnar interactions. At the transition temperature of these ordered columnar phases into the nematic or isotropic phase, different possibilities of losing order may occur depending on the strength of interactions inside a column: In the case of strong hydrogen bonding, the intercolumnar order is lost, whilst the columns themselves persist. A columnar nematic (N_C) phase is formed. If the hydrogen bonds are less strong, the columns break into smaller pieces. Below a certain column lengths, the sample appears to be optical isotropic, although columnar aggregates are still present. If the order inside a column is lost completely, an isotropic phase is obtained, which is disordered on a molecular level.

Results and Discussion

Phase-transitions and liquid-crystalline behavior: Although the thermal data for some of these compounds have been published previously in part,^[2-6,22] we re-measured them to have comparable data that were obtained under identical experimental conditions. The phase transitions, as measured by differential scanning calorimetry (DSC), polarizing optical microscopy (POM), and X-ray diffraction (XRD), are compared in Figure 1. For the transition temperatures, including the enthalpies, see the Supporting Information, section I. Complex polymorphisms, such as solid–solid transitions and plastic crystalline and different LC phases, were observed for many compounds.

The derivatives with a benzene core and linear side-chains of at least six C atoms (**1c–1f**; Figure 1a) exhibited an ordered, columnar, hexagonal, LC phase (Col_{ho} phase). Compounds **1a** and **1b** did not possess LC phases, but rather possessed plastic crystalline mesophases instead. Plastic phases are characterized by a 3D crystal-like order, whilst the molecules within the columns are able to rotate. Therefore, these phases appear to be plastic.^[30–32] Compound **1c** actually showed two hexagonal phases: a plastic Col_{hp} phase followed by a Col_{ho} phase. The temperature range, in which the LC phase was present, became broader with increasing chain length. Whereas the clearing temperatures (T_c) of the LC compounds were located between 207 and 218 °C, independent of the chain length, the melting temperature (T_m) decreased with increasing chain length from 172 °C (**1c**) to 58 °C (**1f**). The DSC heating traces are shown in Figure 2. The temperature range, over which the LC phases were thermodynamically stable, is indicated by horizontal arrows. The textures of the LC phases were recorded upon cooling at the marked temperatures.

Branched benzene tricarboxamides (Figure 1b) were transformed into isotropic liquids at markedly higher temperatures, except for compound **1o**. Their corresponding phase-transition enthalpies were also higher. Branched side-chains stabilized aggregation in the mesophases. Just like their linear analogues, the compounds with four C atoms in

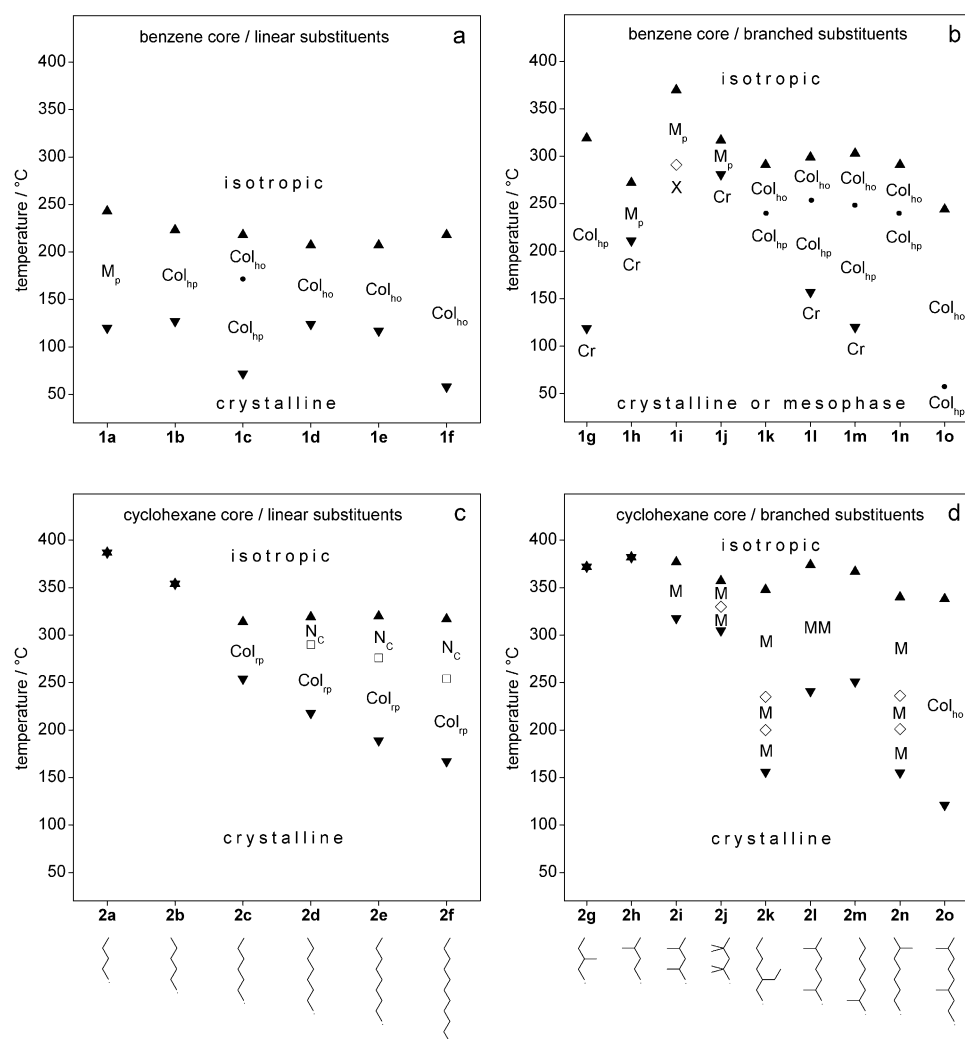


Figure 1. Phase-transition temperature as a function of the substituent and the core (DSC, 1st heating): a) benzene core with linear alkyl substituents; b) benzene core with branched alkyl substituents; c) cyclohexane core with linear alkyl substituents; d) cyclohexane core with branched alkyl substituents. Cr=crystalline, Col=columnar mesophase, h=hexagonal, r=rectangular, p=plastic crystalline, o=ordered liquid crystalline, N_C =columnar nematic, M=unidentified mesophase, X=unknown solid phase (not ordered enough for a crystalline phase). Transitions: crystalline–mesophase (∇), crystalline–isotropic (\star), mesophase–isotropic (\blacktriangle), Col_{hp} – Col_{ho} (\bullet), Col_{rp} – N_C (\square), mesophase–mesophase (\diamond).

the longest side-chain (**1g–1j**) did not show LC behavior but rather showed a plastic crystalline mesophase, which transformed directly into the isotropic phase. Similar to compound **1c**, compounds with longer side-chains (**1k–1o**) showed two Col_h phases: a Col_{hp} phase followed by a Col_{ho} phase. Whilst compound **1o** showed an exceptionally broad Col_{ho} phase between 57 and 244°C, compounds **1k–1n** were liquid crystalline over a smaller range (around 250–300°C). Regarding the temperature of transition into the isotropic state, it was not only important whether the side-chain was branched or linear, but also the position of branching was important: The transition temperatures increased if the branching was closer to the core.

Cyclohexane tricarboxamides with linear alkyl substituents (Figure 1c) showed considerably higher transition temperatures into the isotropic state. In contrast to the aromatic

compounds with linear alkyl substituents, compounds **2c–2f** formed columnar rectangular plastic (Col_{rp}) mesophases followed by nematic LC phases. XRD of compound **2f** revealed that its nematic phase was classified as N_C , which is very uncommon (see below).

Cyclohexane derivatives with branched alkyl substituents (Figure 1d) showed numerous DSC transitions in most cases. Nearly all of these compounds exhibited more than one mesophase and, in some cases, additional crystalline phases were present. The temperatures of transition into the isotropic phase were between 338 and 382°C, which pointed to stronger interactions than in the benzene derivatives. Compound **2o** was the only one that definitely formed a Col_{ho} phase, as known from the aromatic analogues. With a stability range of more than 200 K (121–338°C), compound **2o** shows the broadest LC phase of all of the compounds investigated herein.

As examples of the influence of linear versus branched substituents and benzene versus cyclohexane tricarboxamides, the thermal behavior of compounds **1f**, **1o**, **2f**, and **2o** were compared (Figure 3). Higher temperatures of transition into the isotropic phase were observed for the branched compounds.

The transition temperature of compound **1o** was 26 K higher than that of compound **1f** and that of compound **2o** was 21 K higher than that of compound **2f**. For the cyclohexane tricarboxamides, the clearing temperatures were higher (317 and 338°C for compounds **2f** and **2o**, respectively) than those of the analogous benzene derivatives (281 and 244°C for compounds **1f** and **1o**, respectively). Whilst compounds **1f**, **1o**, and **2o** possessed a broad Col_{ho} phase, compound **2f** showed two crystalline phases followed by a plastic crystalline Col_{rp} phase and a liquid crystalline N_C phase.

Investigation of the mesomorphic state: To use these supramolecular structures in devices or as supramolecular nanofibers, it is of fundamental importance to gain an insight into their molecular arrangement within the different meso-

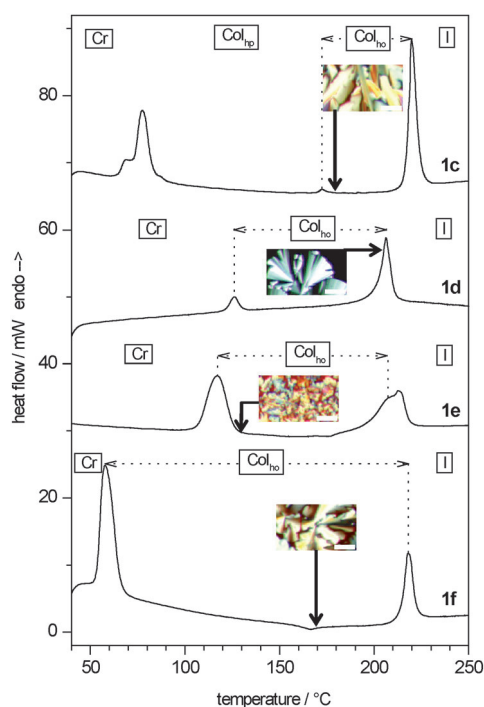


Figure 2. DSC–temperature plots of the first heating scan of linear-substituted benzene tricarboxamides, which indicated the formation of a broader LC phase (\leftrightarrow) and a lower T_m with increasing chain length (**1c–1f**); mesophase textures were recorded under cooling at the indicated temperature, scale bar: 50 μm .

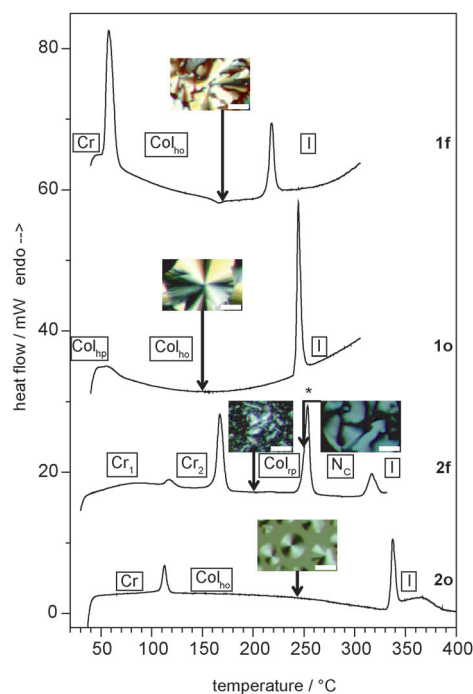


Figure 3. DSC–temperature plots of the first heating scan of linear (**f**) and branched (**o**) benzene (**1**) and cyclohexane (**2**) tricarboxamides showed higher transition temperatures for branched compounds and for the cyclohexane compounds. *: Micrographs of the textures were recorded under cooling at the indicated temperature, scale bar: 50 μm .

phases. Therefore, these compounds were studied by XRD to investigate the interdisc distance and the lateral order and to identify the type of mesophases present. For example, the diffraction patterns of compounds **1o** and **2o**, which both formed a Col_{ho} phase, are shown in Figure 4. The dis-

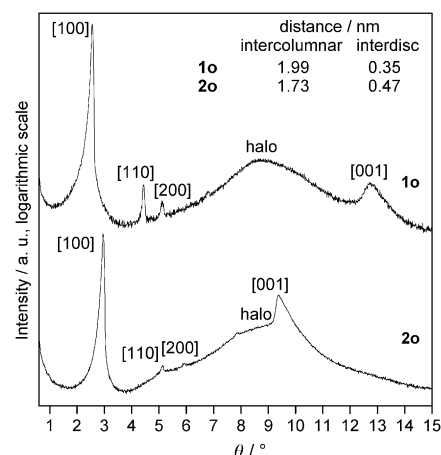


Figure 4. XRD patterns of a benzene tricarboxamide (**1o**) and its analogous cyclohexane derivative (**2o**) in the LC state (Col_{ho}) at 150°C: The cyclohexane derivative showed a smaller lateral distance but a larger interdisc distance. The halo in the wide-angle range was caused by interactions between the amorphous parts without long-range order. Such halos are common in the LC phase, whereas the occurrence of distinct signals in this range pointed to 3D crystalline order.

tance of interdisc spacing [001] rose from 0.35 nm for the benzene core to 0.47 nm for the cyclohexane core, independent of the alkyl substitution pattern (see below). This rise of about one third was due to packing reasons. A hexagonal lattice was characterized by the presence of at least three signals with the ratio of their corresponding lattice distances of $1:1/\sqrt{3}:1/2$, which corresponded to the [100], [110], and [200] spacing, respectively. The column distance was slightly smaller for the alicyclic compounds. The columns packed closer together than the aromatic compounds.

For all of the liquid crystalline benzene tricarboxamides, the LC phase was assigned to be a Col_{ho} phase. The hexagonal arrangement of compound **1o** is shown in Figure 5. The same hexagonal order was also present in the plastic Col_{hp} phase that was formed by several compounds. The core-core distances (a) were calculated with ChemSketch.^[33] The distances between the molecules were drawn such that $a = 1.99$ nm, as obtained from the XRD investigations. Assuming that the side-chains were elongated, they nearly touched the core of the adjacent molecule, which meant that the side-chains interlaced with each other.

The column distance in the hexagonal arrangement was obtained by XRD from the lattice distances that were calculated by using Bragg's law (Figure 6 and Figure 7). The column distances, as well as the interdisc spacing, are listed in the Supporting Information, Table S1. The aromatic compounds that contained linear side-chains (**1b–1f**) showed a linear increase in the column distance of 0.1 nm per addi-

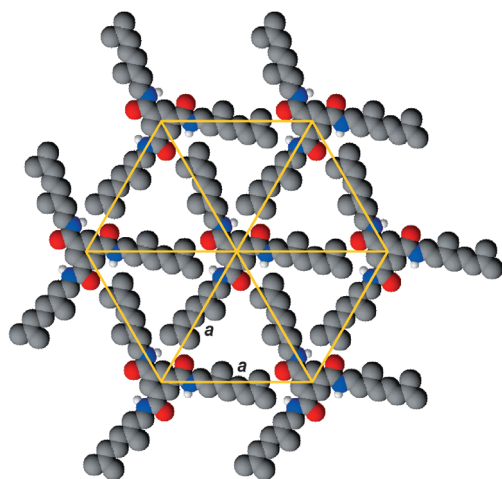


Figure 5. Hexagonal arrangement in a columnar hexagonal phase of compound **1o**; the core–core distances are drawn with the calculated distance of $a = 1.99$ nm, as obtained from the XRD investigations.

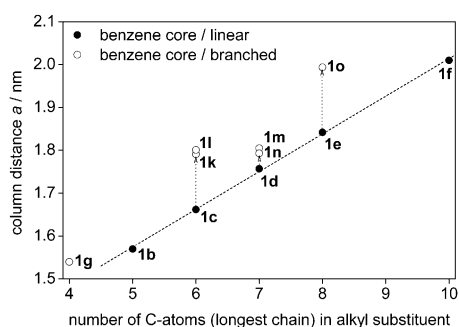


Figure 6. Column distance a (Figure 5) of benzene tricarboxamides in the hexagonal phase at 150 °C: Compounds without branches (●) showed a linear increase with chain length (line); larger spacing was determined for branched compounds (○) with the same main chain length (↑).

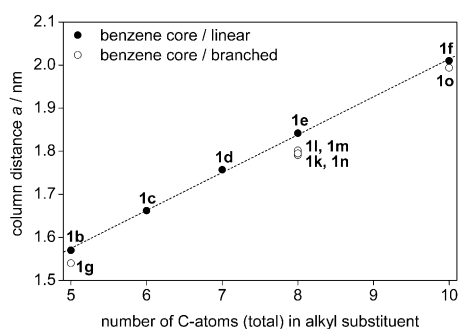


Figure 7. Column distance a (Figure 5) of benzene tricarboxamides in the hexagonal phase at 150 °C versus the total number of C atoms in the side-chain, including branches; the branched compounds (○) needed less space than their elongated analogues (●).

tional C atom, which was independent of the type of Col_h mesophase (Col_{hp} for compounds **1b** and **1c**, Col_{ho} for compounds **1d–1f**) at a fixed temperature of 150 °C for comparison. Comparing compounds with the same main chain length, the branched compounds that formed a hexagonal

phase (Col_{hp} for compounds **1g** and **1k–1n**, Col_{ho} for compound **1o**) showed a larger spacing than the unbranched compounds owing to hindered intercalation (Figure 6). In these compounds, the space consumption increased from 1.66 nm (**1c**) to 1.79 nm (**1k**, ethyl substitution) and 1.80 nm (**1l**, dimethyl substitution). For compounds **1m** and **1n**, which were both methyl-substituted, less additional space was needed. The column distance rose from 1.76 nm (**1d**) to 1.81 nm (**1m**) and 1.80 nm (**1n**). Also, compound **1g** showed a larger distance than the extrapolated value of compound **1a**. The column distance also depended on the position of the substituents. The closer the branching was to the core, the larger the space consumption, which hindered the intercalation of the columns. Comparing the total number of C atoms in the side-chain (including branches), the branched compounds needed less space than their elongated analogues, because they were more compact (Figure 7). For example, compounds **1k–1n**, which had side-chains that were constructed from eight C atoms, showed smaller column distances than unbranched **1e**.

Temperature-dependent XRD patterns of compound **1f** were collected to gain an insight into the morphologies of different phases (Figure 8). At 120, 150, and 180 °C, three

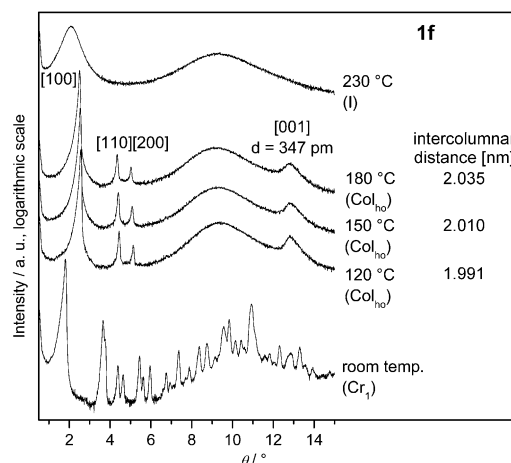


Figure 8. XRD patterns of compound **1f** at different temperatures, which revealed the morphologies in the crystalline, liquid crystalline, and isotropic phases: The pattern at room temperature was measured before heating the sample. A large number of signals were evident for a crystalline phase.

sharp signals in the small-angle range, which corresponded to the [100], [110], and [200] lattice distances, were evidence for a hexagonal phase. The distances increased with temperature owing to thermal expansion of about 0.9 pm K⁻¹. In the wide-angle range, a distinct columnar stacking was shown in the LC phase, with a constant spacing of 347 pm. This signal became weaker at 180 °C, which meant that the columnar order decreased at high temperature. At 230 °C, two diffuse signals pointed to an isotropic liquid with remaining columnar aggregates. If the molecules were totally disordered, no signal would have been observed. The broad diffuse signal at small angles described an average column

distance of about 2.1 nm, which was larger than in the ordered LC phase (21 % larger than at 150 °C). However, the second signal in the wide-angle region, which came from the regular stacking of discs along the column axis, did not appear in the isotropic melt. This result meant that the existing columns were less ordered and/or shorter. The presence of columnar aggregates will be proven later with additional data (see below).

For comparison, a diffraction pattern was collected at room temperature, at which the crystal structure was completely different. No hexagonal order was present, but instead a monoclinic lattice was found with calculated values of $a = 2.48$ nm, $b = 0.70$ nm, $c = 1.23$ nm, and $\beta = 101^\circ$.

The geometries of stacked molecules were simulated for both cores with the same substituent (compounds **1o** and **2o**; Figure 9). The simulated interdisc distances were in very

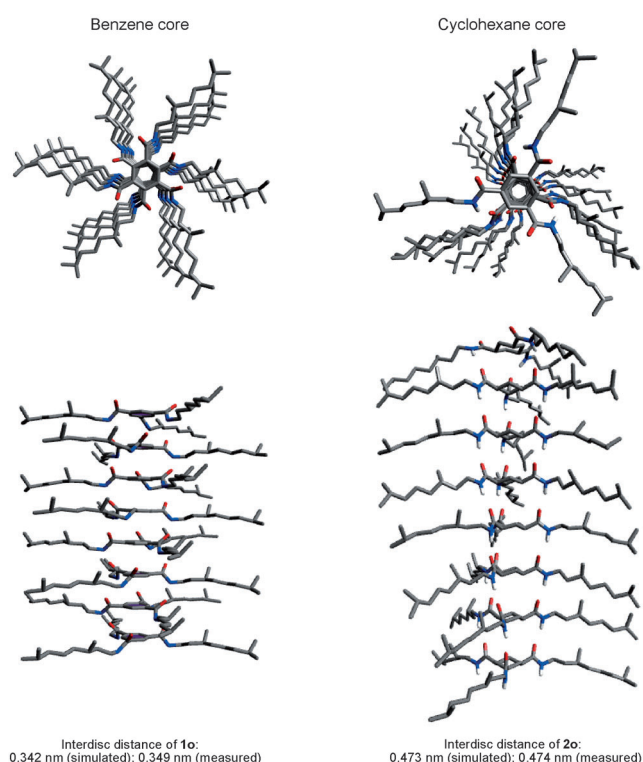


Figure 9. Orthogonal views of the simulated stacking geometries of consecutive molecules within a column for compounds **1o** (benzene core) and **2o** (cyclohexane core); different stacking, depending on the core, led to different interdisc distances for both compounds, which was larger in the case of the cyclohexane core.

good agreement with the results obtained by XRD. The side-chains of consecutive molecules adopted staggered orientations for aromatic compounds and eclipsed orientations for alicyclic compounds. The simulations confirmed the arrangement inside a column, as previously described by Lightfoot et al.^[8] This remarkable difference in packing within a column led to a larger interdisc distance for the cyclohexane derivatives. Because of the eclipsed orientation of their side-chains, the columns of the cyclohexane derivatives

had a noncircular cross-section, which favored a rectangular lattice (Col_r) instead of a hexagonal lattice.^[22]

Investigation of the nematic phase: 1,3,5-Cyclohexanetricarboxamides **2d–2f** formed a nematic phase, which was an intermediate state between the higher-ordered columnar phase and the isotropic liquid. The molecular structure of this nematic phase is of special interest, as it may help to understand what happens at the transition to the isotropic state. Although the existence of this nematic phase has already been described by Tomatsu et al.^[22] for compounds **2d–2f**, the type of nematic phase was not specified. Two different types of nematic phases needed to be considered, namely the discotic nematic (N_D) and columnar nematic (N_C) mesophases.^[29] XRD of compound **2f** in the nematic phase revealed a broad but distinct signal that corresponded to the [001] interdisc distance of 0.47 nm, as also obtained from the higher-ordered columnar phases (Figure 10). In

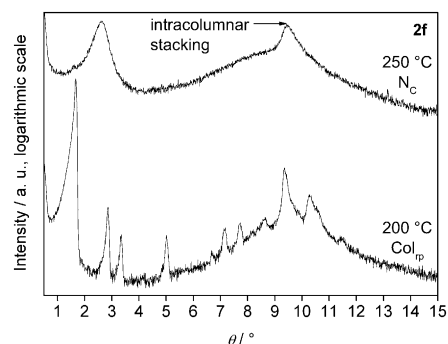


Figure 10. XRD patterns of compound **2f** in the columnar nematic phase (top) and in the columnar rectangular plastic phase (bottom); the signal at around 9.5° showed that intracolumnar stacking was also in the nematic phase.

contrast, in the small-angle range, a broad diffuse signal revealed a liquid-like arrangement of the columns. According to the absence of intercolumnar order and the still-existing intracolumnar spacing, the nematic phase of compound **2f** was classified as N_C . N_C phases are very rare and have only been reported in a few examples. A N_C phase was known to be induced by charge-transfer interactions between a binary mixture of a disk-shaped electron donor and an electron acceptor.^[29,34–36] Such a phase was also found for ionic liquid crystals,^[37] oligomesogens,^[38] bent-core mesogens,^[39] and phthalocyanine complexes.^[40] In contrast to the binary systems and the structurally complex compounds, we observed for the first time, a nematic N_C phase for a single-component system based on a simple molecule. Analogous to compound **2f**, the nematic phases of compounds **2d** and **2e** were also most-likely N_C phases. However, owing to their higher transition temperatures, they were not experimentally investigated by XRD.

Transition from the mesomorphic state into the isotropic state: Herein, we gave special focus on the stepwise losing

of order during heating. Laschat et al. stated that the hexagonal arrangement of columns in discotic liquid crystals was lost in the isotropic melt, although they did not report what happened to the columns themselves.^[29] Therefore, we investigated the transition from the mesomorphic state into the isotropic phase in more detail to obtain an insight into how the order was lost during heating. Coming from 3D order in the crystalline state, columnar hexagonal or rectangular mesophases were formed at higher temperatures, which possessed two types of molecular order: the stacking along the column axis caused by strong threefold hydrogen bonding and weaker 2D lateral order. In this case, the interdisc interactions were several orders of magnitude stronger.^[7] At the upper transition temperature of these ordered columnar phases, there were different possibilities of losing order depending on the strength of interactions inside a column (Figure 11). If the weaker lateral interactions were lost first,

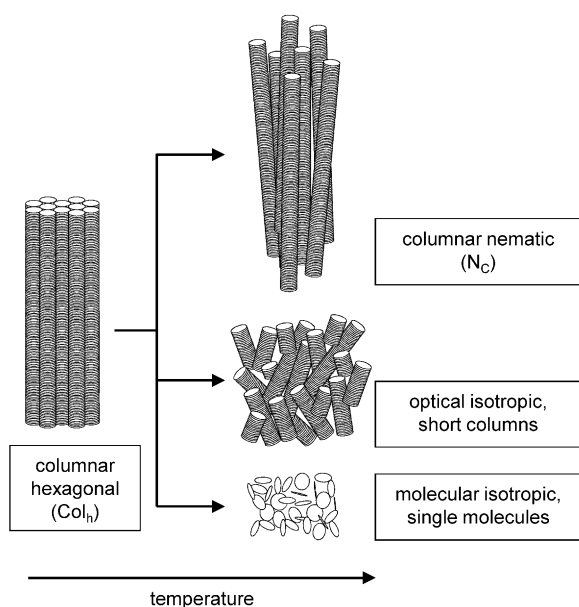


Figure 11. Losing of order during heating: Depending on the strength of the interactions inside a column, an anisotropic columnar nematic phase, an optical isotropic phase that consisted of short columns, or a molecular isotropic phase with disordered molecules was formed.

whilst the hydrogen bonds persisted completely, a columnar nematic (N_C) phase was formed, which appeared optical anisotropic. If the hydrogen bonds were less strong, the columns would break into smaller pieces. Below a certain column lengths, the sample appeared to be optical isotropic. This optical isotropic phase, in which short columns were still present, must be distinguished from the molecular isotropic phase, in which the columnar order was lost entirely. The optical isotropic phase is an intermediate state in between the anisotropic nematic and the molecular isotropic phases.

Infrared (IR) spectroscopy allows the study of changes in H-bonded aggregates by different absorptions of amide

bonds. In the hydrogen-bonded state, the N–H and C=O bonds were weaker and the absorption bands of their vibrations appeared at lower wavenumbers.^[5,41,42] As an example, the $\nu(\text{N–H})$ and $\nu(\text{C=O})$ vibrations of compound **1f** were investigated in the solid state, in solution, and in the optical isotropic melt. The different vibrations were indicated as ν_1 for strongly hydrogen-bonded species, ν_2 for weakly hydrogen-bonded species, and ν_3 for molecularly dissolved species. For compound **1f**, these types of N–H species at different conditions are shown in Figure 12. Vertical lines mark the

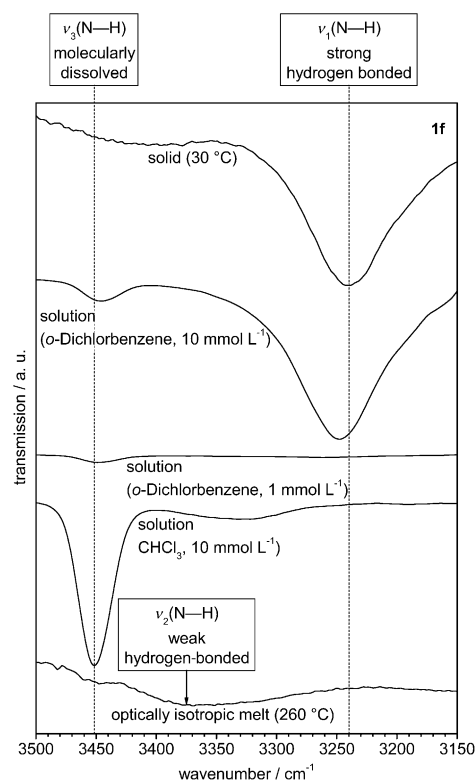


Figure 12. IR spectra of compound **1f** showed strong hydrogen bonds in the solid and partially in 10 mmol L^{-1} *o*-dichlorobenzene solution (ν_1), whereas compound **1f** was molecularly dissolved in dilute *o*-dichlorobenzene as well as in CHCl_3 (ν_3). In the melt, weak hydrogen-bonded aggregates were present (ν_2).

wavenumbers of the absorption maxima of the $\nu_3(\text{N–H})$ absorption and the $\nu_1(\text{N–H})$ absorption. The $\nu_1(\text{N–H})$ absorption at 3240 cm^{-1} , which is typical for strong hydrogen-bonding interactions, was present in the solid state and partially present in 10 mmol L^{-1} *o*-dichlorobenzene. The $\nu_3(\text{N–H})$ absorption at about 3450 cm^{-1} , which indicated the presence of free amide groups, was detected in solution, as would be expected in a molecularly dissolved state. Similar compounds have been reported to be molecularly dissolved in CHCl_3 .^[6,10] In the optical isotropic melt of compound **1f**, the $\nu_3(\text{N–H})$ absorption only occurred very weakly. Instead, another broad absorption band $\nu_2(\text{N–H})$ appeared at 3375 cm^{-1} , which belonged to a weakly hydrogen-bonded species. This absorption was located between the molecular-

ly dissolved and the strongly associated species. Although these hydrogen bonds were weaker than at room temperature, the columnar aggregates were still present in the optical isotropic melt.

The IR spectra of compound **1f** as a function of temperature were collected from 30–290 °C (for the spectra, see the Supporting Information, section II). The absorbance of the strongly bonded amide groups ($\nu_1(\text{N-H})$ and $\nu_1(\text{C=O})$) decreased, whilst the absorbance of the weakly bonded ($\nu_2(\text{N-H})$ and $\nu_2(\text{C=O})$) and the free amide groups ($\nu_3(\text{N-H})$) increased as expected during heating. Figure 13 shows the

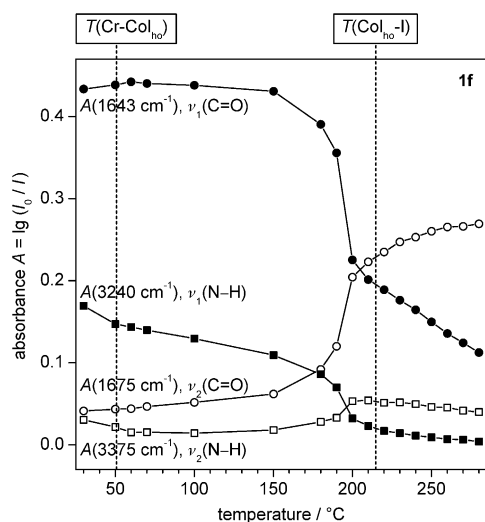


Figure 13. IR absorbance of compound **1f** as a function of the temperature; squares: $\nu(\text{N-H})$, circles: $\nu(\text{C=O})$, filled symbols: strongly hydrogen-bonded species (ν_1), open symbols: weakly hydrogen-bonded species (ν_2); vertical lines: transition temperatures obtained by DSC (first heating, 1 K min⁻¹).

transition from the strongly associated to the weakly associated species. The intensity at the absorption maxima of the vibrations $\nu(\text{N-H})$ and $\nu(\text{C=O})$ for both ν_1 and ν_2 were investigated as a function of temperature. The absorbance (A) was calculated from the IR spectra by using the baseline method.^[43] A is defined as in Equation (1):

$$A = \lg(I_0/I) \quad (1)$$

I_0 and I are the transmission intensities of the beam before and after its transmission through the sample. These relative absorbance values were normalized to the absorbance of the aliphatic $\nu(\text{C-H})$ vibration, which was not involved in the phase-transition and remained constant.

For compound **1f**, no significant change in the absorbance was observed for the transition from the crystalline phase into the columnar hexagonal mesophase. XRD measurements showed that the morphology in the crystalline phase was different to that in the mesophase (Figure 8) with respect to the arrangement of the columns with each other but not with respect to the structure within the columns. At the

melting transition temperature, the monoclinic lattice was transformed into a hexagonal lattice. The corresponding high transition enthalpy only resulted from intercolumnar interactions. Because the stacking inside a column was not affected, no change in H-bonding should be observed. Approximately 15 K below the transition temperature (DSC) from the mesophase into the optical isotropic phase, the absorbance of the $\nu_1(\text{N-H})$ and $\nu_1(\text{C=O})$ vibrations that corresponded to the strongly bonded species decreased, whereas the absorbance of the two $\nu_2(\text{N-H})$ and $\nu_2(\text{C=O})$ vibrations that corresponded to the weakly bonded species increased. In the optical isotropic phase, these changes continued, albeit with a smaller slope. This result confirmed the existence of aggregates that broke up slowly with an increase in temperature.

Similar to compound **1f**, alicyclic compound **2f** also did not show a significant change in the absorbance at the transition from the crystalline phase into the columnar mesophase (Figure 14). At higher temperatures in the range 220–

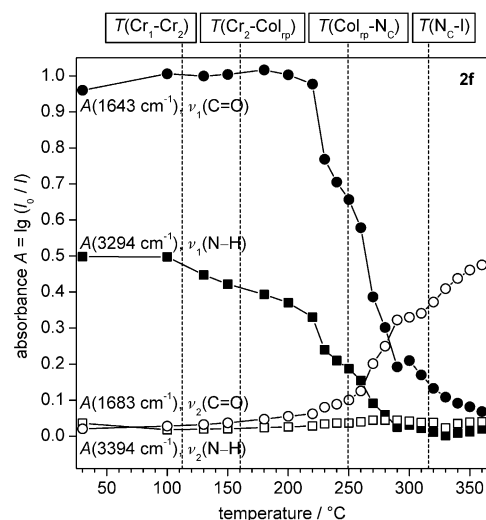


Figure 14. IR absorbance of compound **2f** as a function of the temperature; squares: $\nu(\text{N-H})$, circles: $\nu(\text{C=O})$, filled symbols: strongly hydrogen-bonded species (ν_1), open symbols: weakly hydrogen-bonded species (ν_2); vertical lines: transition temperatures obtained by DSC (first heating, 1 K min⁻¹).

290 °C, the absorbance of both ν_1 vibrations decreased, whereas the absorbance of the two ν_2 vibrations increased. This result correlated with the transition from the Col_{tp} phase into the N_c phase at 249 °C (DSC, 1 K min⁻¹). At this transition, the intercolumnar order was lost and the columns broke into shorter pieces. In contrast to compound **1f**, these pieces were still long enough to form a columnar nematic phase. On further heating, the columns became shorter, thereby resulting in an optical isotropic phase above the clearing temperature at 316 °C (DSC, 1 K min⁻¹). However, the changes in the absorbance continued, with a significantly smaller slope. This result confirmed the slow break-up of aggregates and them becoming shorter with increasing temper-

ature. The absorption of the free amide groups (ν_3) in the melt was not detected for the alicyclic compound (**2f**) in contrast to compound **1f**.

The intercolumnar and intracolumnar interactions cannot be regarded individually, as they influence each other. Obviously, the long columnar aggregates were stabilized by intercolumnar interactions in the mesophases. Within a column, the molecules were stacked and all of the amide groups pointed in the same direction, thereby generating a macrodipole that governed the intermolecular interactions. This phenomenon was described in the literature for tricarboxamides.^[8,12,13,23,24,44] Through a partly antiparallel arrangement of adjacent columns, the dipole moments were compensated and the columnar structure was stabilized.^[9] If the lateral order was lost at the clearing temperature, the columns would become unstable and break into shorter pieces. Only in those cases with exceptionally strong H-bonds would the possibility of the formation of N_C phases exist. At higher temperatures in the optical isotropic melt, there were still columnar aggregates present. The molecules were definitely not disordered on a molecular level.

Brunsveld et al.^[6] reported that the unusually high clearing enthalpy of compound **1o** resulted from the melting of the three intermolecular hydrogen bonds. This result did not agree with our findings that, at T_c , mainly the lateral interactions were lost. Our interpretation was supported by the following example: The amide groups of compounds **1f** and **1o** absorbed at the same wavenumbers in the LC phase as well as in the isotropic phase. Although the energy difference necessary to weaken the hydrogen bonds was the same in both cases, compounds **1f** and **1o** differed from each other in terms of the clearing enthalpy (19 and 31 kJ mol⁻¹ for compounds **1f** and **1o**, respectively). This result meant that the enthalpy difference between compounds **1f** and **1o** could not be explained by the break-up of hydrogen bonds, but by different lateral interactions. In conclusion, the intermolecular H-bonds were only broken up to a small extent into shorter columns.

The presence of columnar aggregates in the optical isotropic phase was also confirmed by XRD measurements. The diffraction pattern of compound **1f** showed a distinct signal at small angles, which corresponded to the columnar distance (Figure 15). The observation of a columnar distance indicated the presence of columnar aggregates in the optical isotropic phase. The diffuse halo in the wide-angle region came from short-range order, which was also present in isotropic phases of small molecules (c.f. the toluene curve, Figure 15). Compound **3** was investigated as a reference compound. Here, the hydrogen atoms of the amide groups were substituted by methyl groups; therefore, compound **3** was not able to build up stable columns through hydrogen bonds. The XRD pattern of compound **3** in the isotropic phase only showed a very weak signal at small angles, thus confirming the absence of columnar aggregates.

Although in the case of compound **1f**, columnar aggregates were present in the optical isotropic melt, no columnar nematic phase was observed. One condition for the appear-

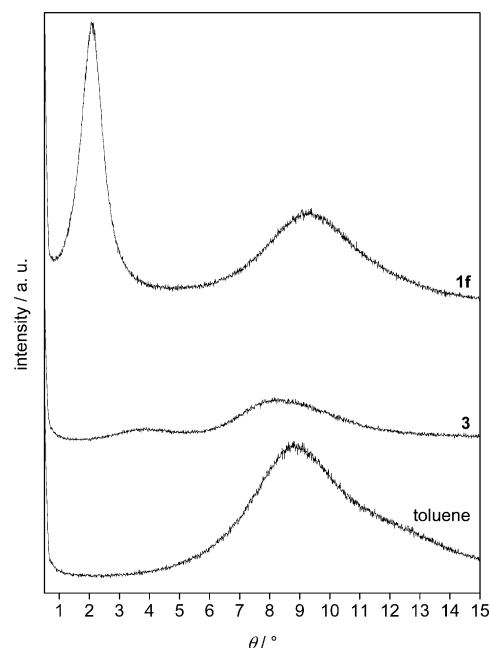
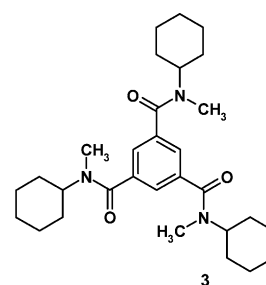


Figure 15. Diffraction patterns from the optical isotropic melts of compound **1f** (230 °C), compound **3** (150 °C), and toluene (RT); the signal of compound **1f** in the small-angle region indicated columnar aggregation.

ance of nematic liquid crystalline phases is an axial ratio (length/diameter) above which rod-like molecules orient themselves along a director. Flory characterized rod-like liquid crystals by their excluded volume. He found that nematic order in a thermotropic system was only stable if the axial ratio was above 6.42.^[45] This theory did not consider macrodipole interactions, which were present in our case. Therefore, the minimum axial ratio might differ for the discussed compounds. The columnar aggregates could be considered as single rod-like molecules; these aggregates were able to form a N_C phase above a certain length. The diameter of a column was estimated by assuming the presence of elongated side-chains and a virtual circle around the molecule. For example, compound **1f** had a diameter of 3.5 nm. To obtain a suitable axial ratio to form a stable nematic phase, a length of the aggregates of more than 22.5 nm corresponded to at least 65 molecules, by taking the measured disc spacing of 0.35 nm into account. Shorter aggregates appeared to be optical isotropic and the interdisc spacing was not present in the XRD pattern. A signal could only be observed for regular spacing above a certain number of repeating units. This optical isotropic phase where short columns

were still present (**1f**) must be distinguished from the molecular isotropic phase (**3**), in which the columnar order was entirely lost.

Conclusion

Two series of 1,3,5-tricarboxamides, one with a benzene core and one with a cyclohexane core, with linear and branched alkyl substituents were compared with respect to their phase behavior and mesophase structure to obtain a deeper understanding of the structure–property relationships in these compounds. Depending on the substituent and the core, a large variety of columnar mesophases were obtained, including columnar hexagonal plastic, columnar rectangular plastic, and columnar hexagonal liquid crystalline phases, as well as a columnar nematic (N_C) phase. N_C phases are very rare and have only been reported in a few examples. For compounds **2d–2f**, we observed for the first time a N_C phase for a single-component system that was based on a simple molecule. Linear-substituted benzene tricarboxamides showed a broader LC-phase with increasing chain length. Branched compounds showed higher transition temperatures into the isotropic phase than their linear analogues. The transition temperatures for cyclohexane tricarboxamides were higher than those for benzene tricarboxamides.

The column distances of the branched aromatic compounds were smaller than their linear analogues in relation to the total amount of C atoms. In the case of a columnar hexagonal mesophase, a smaller column distance was found for the alicyclic compounds compared to the aromatic ones. The interdisc distance was larger for the alicyclic compounds. The stacking geometries in the columnar phases were simulated for both core types with the MOPAC2009 program. The simulated interdisc distances were in very good agreement with the results obtained by XRD.

The columnar hexagonal or rectangular mesophases, which were formed in most cases, possessed two types of molecular order: First, they were stacked along the column axis as a result of strong hydrogen bonding and, second, they showed 2D lateral order between the columns. At the temperature for the transition of ordered columnar phases into phases with lower order, three types were observed depending on the internal strength of the interactions inside the column. In the case of strong hydrogen bonding, the intercolumnar order was lost, whilst the columns themselves persisted and a N_C phase was formed. The N_C phase was only observed within the series that was based on the cyclohexane core. The aromatic derivatives were transformed from a Col_h phase directly into the isotropic phase. In this case, isotropic means optical isotropic, but the molecules were not molecularly disordered. Temperature-dependent XRD and IR spectroscopy measurements revealed that the columnar aggregates were still present above the clearing temperature.

Experimental Section

Methods: The phase-transition temperatures and their corresponding enthalpies were determined by using a Perkin–Elmer Diamond DSC with a heating rate of 10 K min⁻¹. For comparison with the IR data, a heating rate of 1 K min⁻¹ was used. The XRD measurements in the range $\theta = 0.5–15^\circ$ were carried out on a Huber Guinier diffractometer 600 that was equipped with a Huber germanium monochromator 611 to get $Cu_{K\alpha 1}$ radiation ($\lambda = 154.051$ pm). An extra slit diaphragm reduced the broadening of the primary beam owing to scattering in air. A custom-made furnace was integrated into the diffractometer, which allowed investigation at temperatures up to 250°C. The samples were prepared in soda-glass capillaries (1.5–2 mm diameter). IR spectra were collected on a Bio-Rad Digilab FTS-40 that was equipped with a heating device by using KBr pellets. Solution samples were prepared between NaCl plates (layer thickness: 0.5 mm). The geometries of the stacked molecules were optimized by using the PM6 semi-empirical method that was implemented in the MOPAC2009 program,^[46] which was able to describe not only hydrogen bonds, but also π – π interactions.^[47] The reliability of the optimized geometries was checked by calculating the vibrational frequencies, which only gave rise to positive frequencies. For compound **2o**, the theoretical core–core separation was about 498 pm, whilst the H-bond distances were about 214 pm.

Synthesis of tricarboxamides: 1,3,5-tricarboxamides were prepared based on both a benzene and a cyclohexane core. The 1,3,5-benzenetricarboxamides (**1a–1o**) were synthesized from the reaction of 1,3,5-benzenetricarboxylic acid chloride with the corresponding amine in *N*-methylpyrrolidone or THF as the solvent and pyridine or triethylamine as the base. Lithium chloride was added to weaken the hydrogen-bonding interactions during the reaction to improve solubility. The *cis,cis*-1,3,5-cyclohexanetricarboxamides (**2a–2o**) were prepared in an analogous manner, but starting from commercially available *cis,cis*-1,3,5-cyclohexanetricarboxylic acid, which was allowed to react with oxalyl chloride to yield the corresponding trichlorides. For further details regarding the synthesis and characterization of these compounds, see the Supporting Information, sections IV and V.

Acknowledgements

We gratefully acknowledge Sandra Ganzleben and Jutta Failner (Macromolecular Chemistry I, University Bayreuth) for the synthesis of most of the tricarboxamides. We thank Dr. Wolfgang Milius (Inorganic Chemistry I, University Bayreuth) for calculating the unit cell of compound **1f** in the crystalline phase. We would like to acknowledge the financial support by the Deutsche Forschungsgemeinschaft (SFB 840-B8).

- [1] S. Chandrasekhar, B. K. Sadashiva, K. A. Suresh, *Pramana* **1977**, *9*, 471–480.
- [2] Y. Matsunaga, N. Miyajima, Y. Nakayasu, S. Sakai, M. Yonenaga, *Bull. Chem. Soc. Jpn.* **1988**, *61*, 207–210.
- [3] Y. Matsunaga, Y. Nakayasu, S. Sakai, M. Yonenaga, *Mol. Cryst. Liq. Cryst.* **1986**, *141*, 327–333.
- [4] P. J. M. Stals, J. F. Haveman, R. Martín-Rapún, C. F. C. Fitié, A. R. A. Palmans, E. W. Meijer, *J. Mater. Chem.* **2009**, *19*, 124–130.
- [5] P. J. M. Stals, M. M. J. Smulders, R. Martín-Rapún, A. R. A. Palmans, E. W. Meijer, *Chem. Eur. J.* **2009**, *15*, 2071–2080.
- [6] L. Brunsveld, A. P. H. J. Schenning, M. A. C. Broeren, H. M. Jansen, J. A. J. M. Vekemans, E. W. Meijer, *Chem. Lett.* **2000**, *3*, 292–293.
- [7] L. Brunsveld, B. J. B. Folmer, E. W. Meijer, R. P. Sijbesma, *Chem. Rev.* **2001**, *101*, 4071–4097.
- [8] M. P. Lightfoot, F. S. Mair, R. G. Pritchard, J. E. Warren, *Chem. Commun.* **1999**, 1945–1946.

- [9] M. Kristiansen, P. Smith, H. Chanzy, C. Bärlocher, V. Gramlich, L. McCusker, T. Weber, P. Pattison, M. Blomenhofer, H.-W. Schmidt, *Cryst. Growth Des.* **2009**, *9*, 2556–2558.
- [10] K. Hanabusa, C. Koto, M. Kimura, H. Shirai, A. Kakehi, *Chem. Lett.* **1997**, *5*, 429–430.
- [11] Y. Yasuda, E. Iishi, H. Inada, Y. Shiota, *Chem. Lett.* **1996**, *4*, 575–576.
- [12] T. Shikata, Y. Kuruma, A. Sakamoto, K. Hanabusa, *J. Phys. Chem. B* **2008**, *112*, 16393–16402.
- [13] A. Sakamoto, D. Ogata, T. Shikata, O. Urakawa, K. Hanabusa, *Polymer* **2006**, *47*, 956–960.
- [14] N. E. Shi, H. Dong, G. Yin, Z. Xu, S. H. Li, *Adv. Funct. Mater.* **2007**, *17*, 1837–1843.
- [15] A. Bernet, R. Q. Albuquerque, M. Behr, S. T. Hoffmann, H.-W. Schmidt, *Soft Matter* **2012**, *8*, 66–69.
- [16] M. Blomenhofer, S. Ganzleben, D. Hanft, H.-W. Schmidt, M. Kristiansen, P. Smith, K. Stoll, D. Mäder, K. Hoffmann, *Macromolecules* **2005**, *38*, 3688–3695.
- [17] F. Abraham, H.-W. Schmidt, *Polymer* **2010**, *51*, 913–921.
- [18] F. Abraham, S. Ganzleben, D. Hanft, P. Smith, H.-W. Schmidt, *Macromol. Chem. Phys.* **2010**, *211*, 171–181.
- [19] N. Mohmeyer, N. Behrendt, X. Zhang, P. Smith, V. Altstädt, G. M. Sessler, H.-W. Schmidt, *Polymer* **2007**, *48*, 1612–1619.
- [20] D. P. Erhard, D. Lovera, C. v. Salis-Soglio, R. Giesa, V. Altstädt, H.-W. Schmidt, *Adv. Polym. Sci.* **2010**, *228*, 155–207.
- [21] M. L. Bushey, T.-Q. Nguyen, W. Zhang, D. Horoszewski, C. Nuckolls, *Angew. Chem.* **2004**, *116*, 5562–5570; *Angew. Chem. Int. Ed.* **2004**, *43*, 5446–5453.
- [22] I. Tomatsu, C. F. C. Fitié, D. Byelov, W. H. de Jeu, P. C. M. M. Magusin, M. Wübbenhorst, R. P. Sijbesma, *J. Phys. Chem. B* **2009**, *113*, 14158–14164.
- [23] E. Fan, J. Yang, S. J. Geib, T. C. Stoner, M. D. Hopkins, A. D. Hamilton, *J. Chem. Soc. Chem. Commun.* **1995**, 1251–1252.
- [24] A. Sakamoto, D. Ogata, T. Shikata, K. Hanabusa, *Macromolecules* **2005**, *38*, 8983–8986.
- [25] K. Hanabusa, A. Kawakami, M. Kimura, H. Shirai, *Chem. Lett.* **1997**, *5*, 191–192.
- [26] A. Heeres, C. van der Pol, M. Stuart, A. Friggeri, B. L. Feringa, J. van Esch, *J. Am. Chem. Soc.* **2003**, *125*, 14252–14253.
- [27] K. J. C. van Bommel, C. van der Pol, I. Muizebelt, A. Friggeri, A. Heeres, A. Meetsma, B. L. Feringa, J. van Esch, *Angew. Chem. Int. Ed.* **2004**, *43*, 1663–1667.
- [28] A. Friggeri, C. van der Pol, K. J. C. van Bommel, A. Heeres, M. C. A. Stuart, B. L. Feringa, J. van Esch, *Chem. Eur. J.* **2005**, *11*, 5353–5361.
- [29] S. Laschat, A. Baro, N. Steinke, F. Giesselmann, C. Hägele, G. Scalia, R. Judele, E. Kapatsina, S. Sauer, A. Schreivogel, M. Tosoni, *Angew. Chem.* **2007**, *119*, 4916–4973; *Angew. Chem. Int. Ed.* **2007**, *46*, 4832–4887.
- [30] B. Glüsen, W. Heitz, A. Kettner, J. H. Wendorff, *Liq. Cryst.* **1996**, *20*, 627–633.
- [31] J. Kopitzke, J. H. Wendorff, *Chemie in unserer Zeit* **2000**, *34*, 4–16.
- [32] S. K. Prasad, D. S. S. Rao, S. Chandrasekhar, S. Kumar, *Mol. Cryst. Liq. Cryst.* **2003**, *396*, 121–139.
- [33] ACD/ChemSketch, © 1994–2009 Advanced Chemistry Development, Inc., the freeware version is available at www.acdlabs.com.
- [34] K. Praefcke, D. Singer, B. Kohne, M. Ebert, A. Liebmann, J. H. Wendorff, *Liq. Cryst.* **1991**, *10*, 147–159.
- [35] K. Praefcke, D. Singer, M. Langner, B. Kohne, M. Ebert, A. Liebmann, J. H. Wendorff, *Mol. Cryst. Liq. Cryst.* **1992**, *215*, 121–126.
- [36] H. Bengs, O. Karthaus, H. Ringsdorf, C. Baehr, M. Ebert, J. H. Wendorff, *Liq. Cryst.* **1991**, *10*, 161–168.
- [37] F. Artzner, M. Veber, M. Clerc, A.-M. Levelut, *Liq. Cryst.* **1997**, *23*, 27–33.
- [38] A. Grafe, D. Janietz, T. Frese, J. H. Wendorff, *Chem. Mater.* **2005**, *17*, 4979–4984.
- [39] A. Lesac, H. L. Nguyen, S. Narančić, U. Baumeister, S. Diele, D. W. Bruce, *Liq. Cryst.* **2006**, *33*, 167–174.
- [40] O. B. Akopova, N. M. Logacheva, V. E. Baulin, A. Y. Tsvadze, *Russian Journal of General Chemistry* **2008**, *78*, 2118–2124.
- [41] H. Volkmann, *Handbuch der Infrarot-Spektroskopie*, Verlag Chemie, Weinheim, **1972**, pp. 143, 367–371.
- [42] H. Günzler, H. Böck, *IR-Spektroskopie*, Verlag Chemie, Weinheim, **1983**, pp. 226–229.
- [43] M. Hesse, H. Meier, B. Zeeh, *Spektroskopische Methoden in der organischen Chemie*, Georg Thieme Verlag, Stuttgart, New York, **1995**, pp. 65–66.
- [44] C. F. C. Fitié, W. S. C. Roelofs, M. Kemerink, R. P. Sijbesma, *J. Am. Chem. Soc.* **2010**, *132*, 6892–6893.
- [45] P. J. Flory, *Adv. Polym. Sci.* **1984**, *59*, 1–36.
- [46] J. J. P. Stewart, *Stewart Computational Chemistry*, Version 10.055 L.
- [47] J. J. P. Stewart, *J. Mol. Model.* **2008**, *14*, 499–535.

Received: October 12, 2011

Revised: January 16, 2012

Published online: May 31, 2012